The Ribonucleolytic Activity of Angiogenin†

Peter A. Leland,‡ Kristine E. Staniszewski,‡ Chiwook Park,‡,§ Bradley R. Kelemen,‡,|| and Ronald T. Raines*,‡,⊥

Department of Biochemistry and Department of Chemistry, University of Wisconsin−Madison, Madison, Wisconsin 53706

Received September 12, 2001

ABSTRACT: Angiogenin (ANG), a homologue of bovine pancreatic ribonuclease A (RNase A), promotes the growth of new blood vessels. The biological activity of ANG is dependent on its ribonucleolytic activity, which is far lower than that of RNase A. Here, the efficient heterologous production of human ANG in *Escherichia coli* was achieved by replacing two sequences of rare codons with codons favored by *E. coli*. Hypersensitive fluorogenic substrates were used to determine steady-state kinetic parameters for catalysis by ANG in continuous assays. The ANG pH−rate profile is a classic bell-shaped curve, with $pK_1 = 5.0$ and $pK_2 = 7.0$. The ribonucleolytic activity of ANG is highly sensitive to Na^+ concentration. A decrease in Na^+ concentration from 0.25 to 0.025 M causes a 170-fold increase in the value of k_{cat}/K_M. Likewise, the binding of ANG to a tetranucleotide substrate analogue is dependent on [Na^+]. ANG cleaves a dinucleotide version of the fluorogenic substrates with a k_{cat}/K_M value of 61 M^{-1} s^{-1}. When the substrate is extended from two nucleotides to four or six nucleotides, values of k_{cat}/K_M increase by 5- and 12-fold, respectively. Together, these data provide a thorough picture of substrate binding and turnover by ANG.

Embryonic development, wound healing, endometrial proliferation, and many other physiological processes rely on angiogenesis—the growth of new capillaries from an existing capillary network. Accordingly, controlling angiogenic activity offers a means to treat cancer (*3*), as well as vascular, rheumatoid, and other diseases (*4*−*6*). Several human proteins promote angiogenesis (*7*−*9*). Of these proteins, only angiogenin (ANG)[1] is known to have ribonucleolytic activity (*10*) [for recent reviews on ANG, see refs *11*−*13*].

ANG is a 14.4-kDa protein that was first isolated from the conditioned medium of a human adenocarcinoma (*14*). Later, ANG was identified as a component of normal human plasma (*15*). Determination of its amino acid sequence revealed that ANG is a homologue of bovine pancreatic ribonuclease A (RNase A; EC 3.1.27.5) (*16*), which was perhaps the most studied enzyme of the 20th century (*17*). Like RNase A, ANG catalyzes the cleavage of the $P-O^{5'}$ bond in RNA on the 3′ side of pyrimidine residues. The ribonucleolytic activity of ANG has been reported to be 10^4−10^6-fold lower than that of RNase A (*18*, *11*), but nevertheless is essential for its angiogenic activity (*19*, *20*).[2] This finding indicates that ANG is likely to promote angiogenesis by a mechanism distinct from that of other angiogenic factors. As a consequence of its low ribonucleolytic activity, ANG has typically been assayed in a discontinuous manner. The effects of pH and salt concentration on catalysis by ANG have not been analyzed in detail.

Here, we show that expression in *Escherichia coli* of the cDNA for human ANG is limited by codon usage. We overcome this limitation by replacing several rare codons with the corresponding codons favored by *E. coli*. Then, we use a hypersensitive assay to characterize in detail the ribonucleolytic activity of ANG. First, we determine the pH−rate profile for catalysis by ANG. Next, we reveal the contribution of Coulombic interactions[3] to substrate binding and turnover. Specifically, we measure the effect of salt concentration and substrate length on catalysis. In addition, we use fluorescence anisotropy to measure the effect of salt concentration on the binding of ANG to a single-stranded nucleic acid. Together, our data provide a thorough picture

† This work was supported by Grant GM44783 (NIH). P.A.L. was supported by Molecular Biosciences Training Grant GM07215 (NIH) and by a Steenbock/Wharton Fellowship from the Department of Biochemistry. K.E.S. was a Pfizer Undergraduate Summer Fellow in Molecular Biology and a Hilldale Undergraduate/Faculty Research Fellow. B.R.K. was supported by Chemistry−Biology Interface Training Grant GM08506 (NIH).

* To whom correspondence should be addressed at the Department of Biochemistry, University of Wisconsin−Madison, 433 Babcock Dr., Madison, WI 53706-1544. Tel: (608) 262-8588. Fax: (608) 262-3453. E-mail: Raines@biochem.wisc.edu.

‡ Department of Biochemistry.

§ Present address: Department of Molecular and Cell Biology, University of California, Berkeley, 229 Stanley Hall, Berkeley, CA 94720.

|| Present address: Genencor International, Inc., 925 Page Mill Rd., Palo Alto, CA 94304.

⊥ Department of Chemistry.

[1] Abbreviations: ANG, angiogenin; Bis-Tris, bis(2-hydroxyethyl)-iminotris(hydroxymethyl)methane; 4-DABCYL, 4-((4-(dimethylamino)-phenyl)azo)benzoic acid; DEPC, diethyl pyrocarbonate; DTT, dithiothreitol; EDTA, ethylenediaminetetraacetic acid; 6-FAM, 6-carboxyfluorescein; IPTG, isopropyl β-D-thiogalactopyranoside; MES, 2-(*N*-morpholino)ethanesulfonic acid; PAGE, polyacrylamide gel electrophoresis; PCR, polymerase chain reaction; poly(C), poly(cytidylic acid); RNase A, bovine pancreatic ribonuclease A; SDS, sodium dodecyl sulfate; 6-TAMRA, 6-carboxytetramethylaminorhodamine; Tris, tris(hydroxymethyl)aminomethane.

[2] Although RNase A does not promote angiogenesis, RNase A/ANG hybrids can do so (*21*).

[3] We use the term "Coulombic" rather than "electrostatic" to describe the interaction between two point charges. We consider "electrostatic" to be a general term that encompasses Coulombic interactions, hydrogen bonds, and dipole−dipole interactions, and "Coulombic" to be a specific term that refers only to interactions that obey Coulomb's law: $F = q_1q_2/4\pi\epsilon r^2$ (*1*, *2*).

10.1021/bi0117899 CCC: $22.00
Published on Web 01/03/2002

Table 1: Parameters for Cleavage of Fluorogenic Substrates by Angiogenin

	substrate	phosphoryl groups	k_{cat}/K_M (10^3 M^{-1} s^{-1})[a]
1	6-FAM∼rUdA∼6-TAMRA	3	0.061 ± 0.004
2	6-FAM∼(dA)rU(dA)$_2$∼6-TAMRA	5	0.31 ± 0.01
3	6-FAM∼(dA)$_2$rU(dA)$_3$∼6-TAMRA	7	0.72 ± 0.03
4	6-FAM∼(dA)$_3$rU(dA)$_4$∼6-TAMRA	9	0.74 ± 0.03
5	6-FAM∼(dA)rU(dA)$_2$∼4-DABCYL	5	0.20 ± 0.02

[a] Values (±SE) of k_{cat}/K_M were obtained in 0.10 M MES−NaOH buffer (pH 6.0) containing NaCl (0.10 M) except the value for substrate **5**, which was obtained in 0.05 M acetate, 0.05 M MES, 0.1 M Tris buffer (pH 6.0) containing NaCl (0.10 M)

of substrate binding and turnover by this novel angiogenic protein.

EXPERIMENTAL PROCEDURES

Materials. *E. coli* strain DH5α was from Life Technologies (Gaithersburg, MD). *E. coli* strain BL21(DE3) and the pET22b(+) expression vector were from Novagen (Madison, WI). Enzymes used for DNA manipulation were from Promega (Madison, WI) or New England Biolabs (Beverly, MA). Poly(cytidylic acid) [poly(C)] was from Midland Certified Reagent Co. (Midland, TX). The fluorogenic ribonuclease substrates (Table 1) were from Integrated DNA Technologies (Coralville, IA). All other chemicals and reagents were of commercial grade or better and were used without further purification.

DNA oligonucleotides for the polymerase chain reaction (PCR), site-directed mutagenesis, and DNA sequencing were from Integrated DNA Technologies or Life Technologies. The PCR was performed with reagents from PanVera (Madison, WI). DNA sequences were determined with a Sequenase 2.0 kit from United States Biochemicals (Cleveland, OH) or with a BigDye cycle sequencing kit (Perkin-Elmer, Norwalk, CT) and a ABI 377XL Automated DNA Sequencer at the University of Wisconsin−Madison Biotechnology Center.

Instruments. UV absorbance measurements were made with a Cary model 3 spectrophotometer or a Cary 50 Bio spectrophotometer (Varian, Palo Alto, CA). Total fluorescence measurements were made with a QuantaMaster 1 Photon Counting Fluorometer equipped with sample stirring (Photon Technology International, South Brunswick, NJ). Fluorescence anisotropy measurements were made with a Beacon Fluorescence Polarization System (Pan Vera, Madison, WI).

Construction of Plasmid pANG. A cDNA coding for human ANG was a generous gift from Promega. The ANG cDNA was amplified with the PCR and oligonucleotides PAL1 (5′-CCACCGACCCATATGCAGGATAACTCCAGGTACACACAC-3′) and PAL2a (5′-CCAGGGGCCCTCGAGTTACGGACGACGGAAATTGACTG-3′). Oligonucleotide PAL1 incorporated an *Nde*I site (underlined) and, consequently, a methionine codon in the 5′ end of the cDNA. The catalytic and biological activities of Met(−1) ANG are indistinguishable from those of native ANG (*22*). PAL2a incorporates an *Xho*I site (underlined) immediately 3′ to the UAA termination codon. The amplified cDNA fragment was purified with a Wizard PCR purification kit (Promega) and digested with *Nde*I and *Xho*I. The digest product was band-purified and then ligated to the band-purified *Nde*I−*Xho*I fragment of pET22B(+). The integrity of the ANG cDNA was confirmed by determining its sequence.

The ANG cDNA contains two prominent runs of codons that occur with low frequency in the *E. coli* genome. To optimize bacterial expression of the ANG cDNA, these rare codons were replaced with high-frequency *E. coli* codons by site-directed mutagenesis. Oligonucleotide PAL5 (5′-TGAGGTCAGGCC*GCGACGGCG*CATGATGCTTTCA-3′) was used to replace the rare arginine codons 31−33 (^{31}AGG, ^{32}AGA, and ^{33}CGG) with preferred codons for arginine (^{31}CGC, ^{32}CGU, and ^{33}CGC; reverse complements in italics) and to incorporate a silent *Bgl*I site (underlined). Oligonucleotide PAL6 (5′-AGAAGACTTGCT*AATGCG-CAGG*TTTC*GCG*GTGAGGGTTTCCA-3′) was used to replace the rare codons of Arg66, Leu69, Arg70, and Ile71 (^{66}AGA, ^{69}CUA, ^{70}AGA, and ^{71}AUA) with preferred codons for these amino acids (^{66}CGC, ^{69}CUG, ^{70}CGC, and ^{71}AUU; reverse complements in italics) and to incorporate a silent *BspM*I site (underlined). Following mutagenesis, the integrity of the ANG cDNA was confirmed by sequencing. The pET22B(+)-based vector carrying the optimized ANG cDNA was named 'pANG' and was used exclusively for the production of ANG.

Production of ANG from the pET-22b(+)-based vectors was analyzed by SDS−PAGE. Cells (1 mL) from a 20-mL culture were collected immediately prior to and 2 h after induction with IPTG. Pelleted cells were resuspended in 0.2 mL of 0.05 M Tris-HCl buffer (pH 6.8) containing DTT (0.1 M), SDS (2% w/v), bromphenol blue (0.1% w/v), and glycerol (10% v/v). Samples were boiled for 15 min, loaded onto a polyacrylamide (15% w/v) gel, and subjected to electrophoresis. The gel was then stained for 1 h with a filtered solution of EtOH/H_2O/AcOH (5:5:1) containing Coomassie Brilliant Blue R250 (0.1% w/v). The stained gel was then scanned into a computer, and the quantity of ANG in each sample was determined with the program IMAGEQUANT (Molecular Dynamics, Sunnyvale, CA). Pre-induction samples were used to correct the quantitation for proteins that comigrated with ANG.

Production and Purification of Angiogenin. ANG was produced and purified by using methods described previously for RNase A (*23*), with the following modifications. Following expression in *E. coli* strain BL21(DE3) and cell lysis with a French pressure cell, inclusion bodies (containing ANG) were recovered by centrifugation and resuspended in 20 mM Tris-HCl buffer (pH 8.0) containing guanidine hydrochloride (7 M), DTT (10 mM), and EDTA (10 mM). The inclusion bodies were solubilized and denatured by stirring at room temperature for 2 h. The protein solution was then diluted 10-fold with 20 mM AcOH, centrifuged to remove precipitate, and dialyzed overnight versus 20 mM AcOH. Material that precipitated during dialysis was removed by centrifugation. Folding of ANG was initiated by dropwise addition into 0.10 M Tris-HCl buffer (pH 7.8) containing L-Arg (0.5 M), reduced glutathione (3 mM), and oxidized glutathione (0.6 mM) at 4 °C. High concentrations of L-Arg appear to suppress aggregation by enhancing the stability of partially structured folding intermediates (*24*). ANG was then concentrated by ultrafiltration and applied to a Superdex G-75 gel filtration FPLC column (Pharmacia, Pisataway, NJ) that had been equilibrated in 50 mM sodium

acetate buffer (pH 5.0) containing NaCl (0.10 M) and NaN_3 (0.02% w/v). Fractions corresponding to monomeric ANG were pooled and applied to a Mono S cation-exchange FPLC column (Pharmacia). ANG was eluted from the column with a linear gradient of NaCl (0.52−0.62 M) in 20 mM sodium phosphate buffer (pH 7.2).

Trace amounts of any contaminating ribonucleases were removed from ANG by chromatography on a dedicated HiTrap SP cation-exchange column equipped with an LKB peristaltic pump (Pharmacia). All buffers were made with DEPC-treated, distilled and deionized H_2O. Initially, the column was equilibrated with 50 mM sodium phosphate buffer (pH 7.0). The system was then flushed with 20 mL of 50 mM sodium phosphate buffer (pH 7.0) containing NaCl (1.0 M), and again equilibrated with 50 mM sodium phosphate buffer (pH 7.0). ANG (5 mg) in 50 mM sodium phosphate buffer (pH 7.0) was loaded onto the column. The loaded column was washed with 20 mL of 50 mM sodium phosphate buffer (pH 7.0) and then with 35 mL of 50 mM sodium phosphate buffer (pH 7.0) containing NaCl (0.30 M). ANG was eluted from the column with 40 mL of 50 mM sodium phosphate buffer (pH 7.0) containing NaCl (1.0 M). The sample was dialyzed exhaustively against DEPC-treated, distilled and deionized H_2O, concentrated, and aliquoted into 1.7-mL siliconized tubes. ANG concentration was determined by UV spectroscopy using an extinction coefficient of $\epsilon = 0.83$ mL mg^{-1} cm^{-1} at 280 nm, which was calculated with the algorithm of Pace and co-workers (*25*) and is similar to a reported value (*26*).

Zymogram Electrophoresis. Zymogram electrophoresis (*27*−*31*) was used to confirm that purified ANG is free from contaminating ribonucleolytic activity. Briefly, ANG samples were subjected to standard SDS−PAGE (*32*) with the following modifications: the sample buffer did not contain a reducing agent, and the running gel was copolymerized with poly(C) (0.5 mg/mL), which is a substrate for ANG and RNase A. After electrophoresis, SDS was removed from the gel by washing (2 × 10 min) with 10 mM Tris-HCl buffer (pH 7.5) containing 2-propanol (20% v/v). Proteins were renatured by washing the gel for 10 min with 10 mM Tris-HCl buffer (pH 7.5), then for 10 min with 0.10 M Tris-HCl buffer (pH 7.5), and finally for 10 min with 10 mM Tris-HCl buffer (pH 7.5). The gel was stained with 10 mM Tris-HCl buffer (pH 7.5) containing toluidine blue (0.2% w/v) and destained with distilled and deionized H_2O. Toluidine blue stains high-M_r nucleic acids. Consequently, regions in the gel that contain ribonucleolytic activity appear as a clear band in a dark purple background.

Steady-State Kinetic Analyses. Synthetic fluorogenic substrates were used to measure steady-state kinetic parameters (*33*, *34*). The substrates consisted of a single ribonucleotide embedded within a series of deoxyribonucleotides (Table 1). The 5′ end of each substrate was labeled with 6-carboxyfluorescein (6-FAM), and the 3′ end was labeled with 6-carboxytetramethylrhodamine (6-TAMRA; substrates **1**−**4**) or 4-((4-(dimethylamino)phenyl)azo)benzoic acid (4-DABCYL; substrate **5**). When the substrate was intact, 6-TAMRA or 4-DABCYL quenched the fluorescence of 6-FAM. Ribonucleolytic cleavage manifested the fluorescence of 6-FAM.

Assays of ribonucleolytic activity were performed by mixing buffer (2.0 mL) and substrate in a cuvette. To ensure that neither the cuvette nor the buffer was contaminated with a ribonuclease, fluorescence emision at 515 nm with excitation at 490 nm was monitored for 5 min, prior to addition of ANG. After the addition of ANG, cleavage of the fluorogenic substrates was observed by recording fluorescence emission at 515 nm with excitation at 490 nm. Values of k_{cat}/K_M were determined by a linear least-squares regression analysis of the initial fluorescence change using eq 1:

$$k_{cat}/K_M = \left(\frac{\Delta F/\Delta t}{F_{max} - F_0}\right)\frac{1}{[E]} \quad (1)$$

In eq 1, $\Delta F/\Delta t$ is the slope from the linear regression analysis, F_{max} is the maximal fluorescence intensity, F_0 is the initial fluorescence intensity, and [E] is the total enzyme concentration. F_{max} was determined by adding RNase A (∼0.1 μM final concentration) to the reaction mixture after the correlation coefficient (R^2) for the regression analysis of the initial velocity data was greater than 0.99.

pH−Rate Profile for Catalysis. Assays to determine the effect of pH on ANG catalysis were performed in a three-component buffer system containing acetate (0.05 M), MES (0.05 M), and Tris (0.10 M). The buffer pH was adjusted with HCl or NaOH as required. This buffer system maintains a constant ionic strength ($I = 0.10$ M) from pH 4.0 to pH 8.0 (*35*). In addition to the buffer system, reaction mixtures contained NaCl (0.10 M), substrate **5** (20 nM), and ANG (0.47 μM). Substrate **5** (Table 1) has 6-DABCYL as the quenching moiety. Unlike 6-TAMRA, 6-DABCYL is chemically stable at acidic pH and is therefore better suited for the determination of pH-rate profiles (*33*, *34*). Assays with RNase A were also performed with substrate **5** in buffers that likewise contained NaCl (0.1 M) (*34*). Data for ANG and RNase A were fitted to eq 2, which describes the participation of two titratable residues in catalysis:

$$(k_{cat}/K_M)_{obs} = \frac{(k_{cat}/K_M)_{INT}}{\frac{[H^+]}{K_1} + 1 + \frac{K_2}{[H^+]}} \quad (2)$$

In eq 2, $(k_{cat}/K_M)_{obs}$ is the observed k_{cat}/K_M, $(k_{cat}/K_M)_{INT}$ is the intrinsic value of k_{cat}/K_M, K_1 is the acid dissociation constant for the first titratable residue, and K_2 is the acid dissociation constant for the second titratable residue. The value of $(k_{cat}/K_M)_{obs}$ at each pH was determined with eq 1 as described above.

Salt−Rate Profile for Catalysis. Assays to determine the effect of $[Na^+]$ on ANG catalysis were performed at 25 ± 1 °C in 1 mM Bis-Tris buffer (pH 6.0) containing NaCl (25 mM-0.25 M), substrate **2** (6 nM), and ANG (47 nM). Values of k_{cat}/K_M were determined at seven Na^+ concentrations. We used eq 3 (*36*) to describe the dependence of ANG catalysis on $[Na^+]$:

$$(k_{cat}/K_M)_{obs} = (k_{cat}/K_M)^{\ominus}[Na^+]^{-n'} \quad (3)$$

In eq 3, $(k_{cat}/K_M)_{obs}$ is the observed k_{cat}/K_M at each Na^+ concentration, $(k_{cat}/K_M)^{\ominus}$ is the value of k_{cat}/K_M when $[Na^+] = 1.0$ M, and n' describes the dependence of catalysis on $[Na^+]$. This equation is analogous to an equation used by Record and co-workers to describe the effect of $[Na^+]$ on the binding of DNA ligands to proteins (*37*). These authors show that the slope of a log K_d versus log $[Na^+]$ plot provides

a quantitative measure of the number of ion pairs formed between a DNA ligand and a protein. Their analysis is, however, limited to the interactions between polyelectrolytes (>18 DNA monomer units) and proteins (*38*). Substrate **2**, which was used to determine the ANG salt−rate profile, is a tetranucleotide (Table 1). Hence, the value of n' calculated with eq 3 does not provide a quantitative measure of the number of ion pairs between ANG and substrate **2**. Nonetheless, comparison of the values of n' determined for ANG and those calculated for other pancreatic-type ribonucleases under similar conditions provides a measure of the relative importance of Coulombic interactions in catalysis by the various enzymes.

Substrate Dependence of Catalysis. Substrates **1**−**4** (Table 1), which include three, five, seven, or nine phosphoryl groups, respectively, were used to measure the effect of substrate length on ANG catalysis. Assays were performed at 25 ± 2 °C in 0.10 M MES−NaOH buffer (pH 6.0) containing NaCl (0.10 M), substrate (4−60 nM), and ANG (0.47 μM). Values of k_{cat}/K_M were calculated with eq 1 and are the average of duplicate or triplicate determinations for each substrate.

DNA Binding. Fluorescence anisotropy was used to measure the binding affinity of fluorescein-labeled single-stranded DNA, which serves as a substrate analogue, to ANG. Here, we used a tetranucleotide with a 5′-fluorescein label [6-FAM∼d(AUAA)]. The concentration of 6-FAM∼d(AUAA) was 5 nM. Fluorescence anisotropy was measured at 25 ± 2 °C in 10 mM MES−NaOH buffer (pH 6.0) containing NaCl (0.02 or 0.10 M) as described previously (*39*). Data collected at 0.10 M NaCl were fitted to eq 4:

$$A = \frac{\Delta A \cdot [\text{Ang}]}{K_d + [\text{Ang}]} + A_{min} \quad (4)$$

In eq 4, A is the measured fluorescence anisotropy, ΔA is the total change in anisotropy, and A_{min} is the anisotropy of the unbound tetranucleotide (*39*). Equation 4 describes binding at a single specific site. Yet, at 0.02 M NaCl and high [ANG], the substrate analogue also binds nonspecifically to ANG. Therefore, data collected at 0.02 M NaCl were fitted to eq 5, which includes a term (K_{ns}·[ANG]) to describe nonspecific binding:

$$A = \frac{\Delta A \cdot [\text{Ang}]}{K_d + [\text{Ang}]} + A_{min} + K_{ns} \cdot [\text{Ang}] \quad (5)$$

RESULTS

Production and Purification of Angiogenin. Our initial attempts to produce human ANG from a pET-22b(+)-based vector yielded less than 2 mg of pure protein per liter of *E. coli* culture medium. The ANG mRNA has multiple codons that are disfavored by *E. coli*. In two instances, these rare codons are sequential. The codons for Arg31, Arg32, and Arg33 occur with a multiplicative frequency of less than <0.5% (*40*). When these rare codons are replaced with the arginine codons favored by *E. coli*, the amount of ANG in crude cell extracts increases by 4.0-fold (Figure 1). The codons for Arg66, Leu69, Arg70, and Ile71 occur with a multiplicative frequency of <0.4% (*40*). When these rare codons are exchanged for the corresponding favored codons, the amount of ANG in crude cell extracts increases by 2.2-fold compared to that from the native cDNA. Finally, when both sets of codon substitutions are incorporated in a single cDNA, the amount of ANG in crude cell extracts increases by 4.2-fold compared to that from the native ANG cDNA. The plasmid bearing this new cDNA, pANG, was used exclusively for production of ANG.

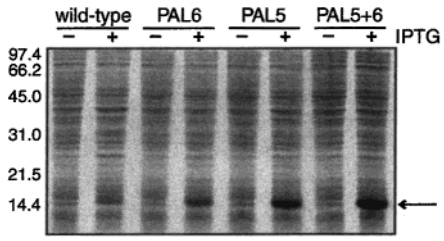

FIGURE 1: SDS−PAGE of *Escherichia coli* lysates harboring a pET-22b(+)-based plasmid that directs the expression of human angiogenin. Cell lysates were prepared immediately prior to addition of IPTG (−) and 2 h after addition of IPTG (+). M_r values from standards are shown. Lanes 1 and 2: Plasmid encoding wild-type human angiogenin. Lanes 3 and 4: Plasmid PAL6 in which codons for Arg66, Leu69, Arg70, and Ile71 of angiogenin are replaced with favored *E. coli* codons. Lanes 5 and 6: Plasmid PAL5 in which codons for Arg31, Arg32, and Arg33 are replaced with favored *E. coli* codons. Lanes 7 and 8: Plasmid PAL5+6 (i.e., pANG) in which both sets of codons are replaced with favored *E. coli* codons. Angiogenin migrates as a 14.4-kDa band (arrow).

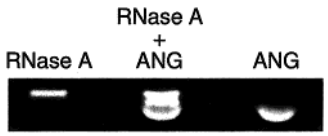

FIGURE 2: Zymogram electrophoresis of angiogenin and ribonuclease A. Lane 1, ribonuclease A (0.25 ng); lane 2, ribonuclease A (0.25 ng) and angiogenin (8 μg); lane 3, angiogenin (8 μg).

After induction of expression with IPTG, ANG accumulated in inclusion bodies in *E. coli* cells. The inclusion bodies were isolated, and their component proteins were reduced, denatured, folded, and applied to a gel filtration column. Monomeric ANG represented the major peak on the chromatogram. Fractions containing ANG were then applied to a cation-exchange column. ANG eluted as a defined peak. Preparations used to measure kinetic parameters were applied to a second, dedicated cation-exchange column to remove trace amounts of any contaminating ribonucleases. Following chromatography, ANG migrates as a single band of appropriate M_r during SDS−PAGE. The production and purification protocol yields approximately 20 mg of purified ANG per liter of *E. coli* culture medium.

Zymogram Electrophoresis. Zymogram electrophoresis (*27*−*29, 31*) is an extraordinarily sensitive means to assay ribonucleolytic activity. This technique can detect the ribonucleolytic activity of 1 pg (10^{-16} mol) of RNase A. Zymogram electrophoresis is also an excellent method to detect contaminating ribonucleolytic activity in preparations of ANG, as RNase A (13.7 kDa) actually migrates more slowly during SDS−PAGE in the absence of a reducing agent than does ANG (14.4 kDa) (Figure 2). Most significantly, ANG migrates as a single band during zymogram electrophoresis. This result indicates that ANG prepared as described herein is free from contaminating ribonucleolytic activity.[4]

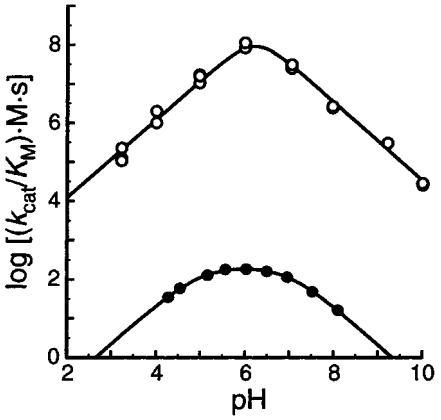

FIGURE 3: Dependence of k_{cat}/K_M values for catalysis by angiogenin and ribonuclease A on pH. Values for angiogenin (●) were determined at 25 °C in a three-component buffer system (0.05 M acetate, 0.05 M MES, 0.10 M Tris) containing NaCl (0.10 M). Values of k_{cat}/K_M for cleavage of substrate **5** at each pH were calculated with eq 1 and fitted to eq 2. Values for ribonuclease A (○) were determined likewise, but with different buffers containing NaCl (0.10 M) (*34*). From eq 2, ribonuclease A: $pK_1 = 6.0$, $pK_2 = 6.4$ (*34*); angiogenin: $pK_1 = 5.0$, $pK_2 = 7.0$.

pH−Rate Profile for Catalysis. The ANG pH−rate profile was determined by measuring k_{cat}/K_M values for substrate **5** as a function of pH. The k_{cat}/K_M values were fitted to eq 2 which describes catalysis by an enzyme with two titratable active-site residues: one that must be protonated and a second that must be unprotonated for catalysis to occur. Like that determined previously for RNase A (*41, 42*), the ANG pH−rate profile is bell-shaped with a maximum near pH 6 (Figure 3). But unlike that of RNase A, the ANG pH−rate profile has a wide plateau. The values of the ANG acid dissociation constants are 5.0 and 7.0. In contrast, these values for RNase A are 6.0 and 6.4 (*34*). The errors on the ANG values, determined by curve fitting, are <1%; the errors determined from duplicate experiments are near 6%. The value of the ANG pH-independent k_{cat}/K_M is 220 M^{-1} s^{-1}.

Salt−Rate Profile for Catalysis. The effect of salt on catalysis by ANG was determined by measuring k_{cat}/K_M values for substrate **2** as a function of Na^+ concentration in 1 mM BisTris-HCl buffer (pH 6.0). A low buffer concentration was used to minimize inhibition caused by any low-level contaminants in the buffer. The effect of such contaminants is minimal at high salt concentrations, but can be pronounced at low salt concentration (*36, 43*). The k_{cat}/K_M values for ANG-catalyzed cleavage of substrate **2** increase from 71 M^{-1} s^{-1} at 0.25 M NaCl to 1.2×10^4 M^{-1} s^{-1} at 0.025 M NaCl (Figure 4). The value of n', which is calculated with eq 3, is 2.3 ± 0.1.

Substrate Dependence of Catalysis. To measure the effect of substrate length on ANG catalysis, we used a series of related fluorogenic substrates (Table 1). As reported previously (*33*), the values of k_{cat}/K_M for RNase A acting on substrates **1**−**4** range from 2.5×10^7 M^{-1} s^{-1} for substrate **1** to 4.8×10^7 M^{-1} s^{-1} for substrate **4**, a modest 2-fold change (Figure 5). In contrast, the range of k_{cat}/K_M values for ANG-catalyzed cleavage of substrates **1**−**4** is significantly larger (Figure 5 and Table 1). Dinucleotide substrate **1** has the lowest value of k_{cat}/K_M at 61 M^{-1} s^{-1}. ANG acts on tetranucleotide substrate **2** with a k_{cat}/K_M value of 310 M^{-1} s^{-1}, a 5-fold increase relative to that for substrate **1**. The value of k_{cat}/K_M for substrate **3**, a hexanucleotide, at 720 M^{-1} s^{-1} is 12-fold greater than that for substrate **1**. The k_{cat}/K_M value for substrate **4**, an octanucleotide, is 740 M^{-1} s^{-1} and is within error of that for substrate **3**.

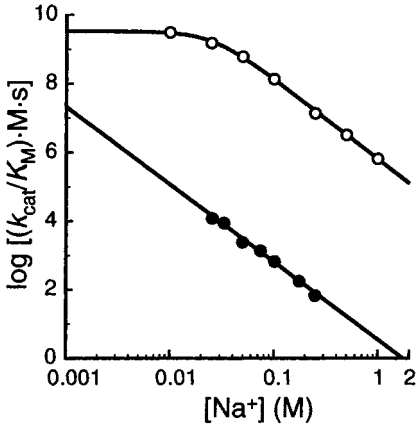

FIGURE 4: Dependence of k_{cat}/K_M values for catalysis by angiogenin and ribonuclease A on Na^+ concentration. Determinations were made at 25 °C in 1 mM Bis-Tris buffer (pH 6.0) containing NaCl (25 mM−0.25 M for angiogenin and 1.0 mM−1.0 M for ribonuclease A). Values of k_{cat}/K_M for cleavage of substrate **2** by angiogenin (●) at each [Na^+] were calculated with eq 1 and fitted to eq 3. Values for ribonuclease A (○) were determined likewise (*36*).

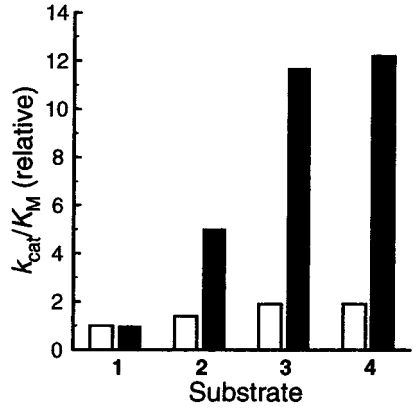

FIGURE 5: Dependence of k_{cat}/K_M values for catalysis by angiogenin and ribonuclease A on substrate length. Values of k_{cat}/K_M are relative to that determined for cleavage of the dinucleotide substrate **1**, which contains three phosphoryl groups, and are the average of duplicate or triplicate determinations. Cleavage of the nucleotide substrates by angiogenin (filled bars) was measured at 25 °C in 0.10 M MES−NaOH buffer (pH 6.0) containing NaCl (0.10 M). Values for ribonuclease A (open bars) were determined likewise (*33*).

DNA Binding. Fluorescence anisotropy was used to measure the effect of Na^+ on the binding of a substrate analogue to ANG. The fluorescein-labeled DNA oligonucleotide 6-FAM∼d(AUAA) had been used previously to measure the binding of single-stranded nucleic acid to RNase A and several variants (*39, 44, 45*). As reported, the value of K_d for the RNase A−6-FAM∼d(AUAA) complex is dependent on [Na^+] (*39, 44, 45*). Similarly, the interaction between ANG and the 6-FAM∼d(AUAA) oligonucleotide is dependent on [Na^+]. At 0.024 M Na^+, 6-FAM∼d(AUAA)

[4] The absence of contaminating RNase A in the ANG preparation is substantiated further by other results reported herein, particularly the distinct active-site pK_a values and the markedly different dependencies of catalysis on substrate length.

forms a complex with ANG that has a K_d value of 6.6 μM. Increasing the [Na^+] weakens binding significantly—at 0.142 M Na^+, the value of K_d for the ANG−6-FAM∼d(AUAA) complex is 0.49 mM.

DISCUSSION

Angiogenin Production and Purification. Pancreatic-type ribonucleases are highly amenable to heterologous production as inclusion bodies in *E. coli*. Previously, we used the T7 RNA polymerase expression system (*46*) to produce RNase A (*31*), bovine seminal ribonuclease (*47*), human pancreatic ribonuclease (*48*), and Onconase (*23*). Folding in vitro and purification have consistently yielded ≥20 mg of fully active ribonuclease per liter of culture medium.

Surprisingly, when we attempted to use the T7 RNA polymerase system for the heterologous production of ANG, it was not possible to purify a significant quantity of ANG. Because the T7 RNA polymerase system produces mRNA with high efficiency, we suspected that inefficient translation was limiting the production of ANG. Analysis with the program RNA FOLD (Genetics Computer Group, Madison, WI) indicated that the start codon and Shine−Delgarno sequence were accessible to the translation machinery (data not shown). Inspection of the cDNA for human ANG revealed, however, two prominent sequences of codons that are disfavored by *E. coli*. The effect of rare codons on the production of foreign proteins in *E. coli* is highly variable and is largely dependent on their context within the mRNA. The rare AGA and AGG arginine codons are often associated with errors that cause premature termination of translation (*49*−*51*).

When the AGG and AGA codons for Arg31 and Arg32, as well as the rare CGG codon for Arg33, are replaced with corresponding high-use codons, the production of ANG increases (Figure 1). Likewise, when the sequence of rare codons from amino acid residues 66−71, which includes two AGA arginine codons, is replaced with corresponding favored codons, the production of ANG increases. Combining both sets of codon substitutions into a single cDNA results in a modest additional increase in production of ANG, compared to that from the cDNA with codon substitutions restricted to amino acid residues 31−33. The use of a codon-optimized cDNA in the T7 RNA polymerase system consistently yields 20 mg of pure ANG per liter of *E. coli* culture medium. In contrast, expression of a synthetic cDNA with a *trp* promoter yields only 2 mg of purified ANG per liter of culture medium (*22*). Recently, a *tac* promoter was used to direct soluble ANG into the periplasm of *E. coli* (*52*). The yield of purified ANG was similar to that reported herein.

pH−Rate Profile for Catalysis. The ANG pH−rate profile is a classic bell-shaped curve (Figure 3). The pH dependence of catalysis is consistent with a mechanism in which two residues, one protonated and the other unprotonated, effect catalysis (Figure 6). By analogy to the RNase A transphosphorylation reaction, ANG residue His13 likely acts as a base to abstract a proton from the 2′-oxygen, and thereby facilitates its attack on the phosphorus atom. ANG residue His114 likely acts as an acid that protonates the 5′-oxygen to facilitate its displacement (*17*). As expected from this mechanism, the H13A and H114A variants of ANG are ineffective catalysts (*20*).

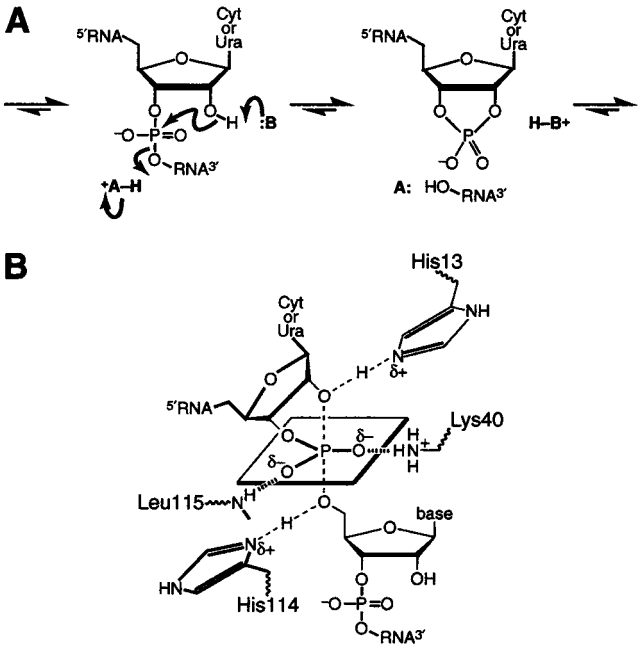

FIGURE 6: (A) Putative mechanism of the transphosphorylation reaction catalyzed by angiogenin. "**B**" is His13, and "**A**" is His114. (B) Putative structure of the transition state during the transphosphorylation reaction catalyzed by angiogenin. The structure is based on the three-dimensional structure of crystalline angiogenin (*56*), and is by analogy to the putative structure of the transition state during the transphosphorylation reaction catalyzed by ribonuclease A (*17*).

Unlike the RNase A pH−rate profile, the ANG pH−rate profile has an obvious plateau (Figure 3). The pK_a values calculated for the active-site histidine residues of ANG are separated by 2 pH units, with pK_1 = 5.0 and pK_2 = 7.0. The acid dissociation constants determined in the same manner for RNase A differ by only 0.4 pH unit, with pK_1 = 6.0 and pK_2 = 6.4 (*36*). Because pK_1 and pK_2 are macroscopic parameters, it is not possible to assign a pK_a value to a particular active-site histidine. The pK_a values for the active-site histidine residues of ANG and RNase A have been measured with NMR spectroscopy. In unliganded RNase A, His12 is slightly more acidic than is His119 (*53*, *54*). This situation favors a protonation state that is appropriate for catalysis of the transphosphorylation reaction. Surprisingly, the pK_a values of the active-site histidine residues in unliganded Ang are inverted—His114 is more acidic than is His13 (*55*). His8, which forms a hydrogen bond with Gln12 [$N^{\epsilon 2}\cdots O^{\epsilon 1}$ distance of 2.8 Å (*56*)] and is not conserved in RNase A, could contribute to the difference in the two pH−rate profiles in Figure 3.

Salt−Rate Profile for Catalysis. The ribonucleolytic activity of ANG depends strongly on [Na^+] (Figure 4). This finding is consistent with Coulombic interactions between cationic subsites of ANG and the anionic substrate being important for binding. Consistent with this conclusion, Shapiro and co-workers have shown than the K_i values of 3′,5′-ADP and 5′-ADP, which have two phosphoryl groups, are 6-fold lower than that of 5′-AMP, which has one (*57*). Similarly, addition of a 3′-phosphoryl group to CpA increases its k_{cat}/K_M value by 9-fold (*57*).

When the chemical transition state limits the rate of catalysis, the value of n' in eq 3 reports on the extent of Coulombic interactions between the enzyme and the substrate

in the chemical transition state (*36*). The low k_{cat} value that has been measured for CpA cleavage by ANG suggests that ANG catalysis is indeed limited by chemistry (*58*). The value of n' for ANG is 2.3 when catalysis is measured with substrate **2**. The salt−rate profile for wild-type RNase A cannot be compared directly with that of ANG because chemistry only partially limits RNase A catalysis (*36*). Rather, Coulombic interactions between RNase A and substrate **2** are best described by the salt−rate profile of K41R RNase A (*36*). The K41R substitution in RNase A does not change the Coulombic interactions between the enzyme and the substrate, but diminishes turnover such that chemistry limits catalysis (*59*). The value of n' for K41R RNase A is 2.7 when catalysis is measured with substrate **2** (*36*). RNase A residues Lys7, Arg10, and Lys66 interact with the phosphoryl groups of a bound substrate (*39*). When all of these residues are changed to an alanine, the value of n' is reduced to 1.4 (*36*). Thus, the n' value for ANG is similar but slightly less than that of K41R RNase A, indicating that the Coulombic interactions between RNase A and substrate **2** are largely but not completely conserved in ANG.

Kinetic and structural studies, as well as comparisons to RNase A, have been used to define the phosphoryl group binding sites of ANG. In RNase A, four enzymic subsites [P(−1), P0, P1, and P2] interact with the phosphoryl groups of a bound substrate (*44, 60*). The P1 subsite is the active site where cleavage of the P−$O^{5'}$ bond occurs. The P0 and P2 subsites bind the phosphoryl groups on the 5′ side and 3′ side of the scissile phosphodiester bond, respectively. The P(−1) subsite of RNase A, which binds the second phosphoryl group on the 5′ side of the scissile phosphodiester bond, was described only recently (*44*). The ANG P1 subsite is similar to that of RNase A (*56, 61*). Kinetic studies support the presence of a P2 subsite in ANG (*57*). The amino acid residues that contribute to the P2 subsite of ANG are, however, distinct from those that contribute to the analogous subsite of RNase A. ANG appears to lack a P0 subsite (*57, 62*), and its absence could account for the slightly lower value of n'.

DNA Binding. Previously, we showed that fluorescence anisotropy is a useful technique to assay complex formation between RNase A and a substrate analogue (*39, 44, 45*). Here, we have used this technique to quantitate substrate binding to ANG. The affinity of ANG for the 6-FAM∼d(AUAA) oligonucleotide is dependent on [Na^+]. A 6-fold change in [Na^+] caused a 75-fold change in the K_d values. The value of K_d determined for ANG−6-FAM∼d(AUAA) complex at 0.142 M Na^+ (K_d = 0.49 mM) is somewhat greater than that reported previously for RNase A and an identical oligonucleotide (K_d = 88 μM) (*45*). Still, the dependence of the K_d values on [Na^+] for RNase A is notably similar to that measured for ANG—an 8-fold change in [Na^+] results in a 100-fold decrease in the value of K_d for the RNase A−6-FAM∼d(AUAA) complex (*45*). These data suggest that ANG and RNase A use Coulombic interactions to a similar extent to bind a substrate. This conclusion is consistent with the similar values of n' derived from salt−rate profiles of catalysis by ANG and K41R RNase A (vide supra).

Substrate Length Dependence. Catalysis by ANG shows a strong dependence on the length of its substrate (Figure 5). This result supports the significance of peripheral subsites in catalysis by ANG. As described above, catalysis by ANG appears to be limited by chemistry. As the length of the substrate molecule increases, the binding energy also increases. Greater binding energy, in turn, results in uniformly greater stabilization of all enzyme-bound species, including the rate-limiting transition state (*63*). Thus, the greater binding energy afforded by a longer substrate is manifested in greater catalytic activity. Although substrate **4** is two nucleotides longer than is substrate **3**, the values of k_{cat}/K_M are approximately equal. Apparently, the additional nucleotides of substrate **4**, compared to substrate **3**, are unable to participate in interactions that enhance catalysis. Unlike ANG, RNase A does not discriminate between substrates **1**−**4** (Figure 5). Catalysis by RNase A is not limited by chemistry alone (*36*), and the enhanced binding energy provided by a longer substrate on RNase A catalysis does not increase the value of k_{cat}/K_M.

Conclusions and Prospectus. A distinctive property of ANG is its markedly low ribonucleolytic activity compared to that of RNase A. The properties of the active-site histidine residues, phosphoryl group binding sites, and nucleobase binding sites likely contribute to the low catalytic activity of ANG. Our data, however, suggest that these features cannot account in total for the difference in catalytic activity between ANG and RNase A. What then is the basis of the inefficiency of ANG as a catalyst of RNA cleavage? It is possible that the orientation of the catalytic residues of ANG (His13, Lys40, and His114) is not optimal for cleavage of the substrates commonly used for measurement of ribonucleolytic activity. Recently, Acharya, Shapiro, and co-workers described the structure of crystalline ANG at 1.8 Å resolution (*56*). In their comparison of the ANG structure to that of the RNase A−uridine 2′,3′-cyclic vanadate complex, these workers noted subtle changes to the positions of the ANG active-site residues compared to their RNase A counterparts.

The physiological substrate of ANG is still unknown. It is unlikely that ANG has a specific recognition sequence for catalysis. Instead, the target may have a specific secondary structure, such as a hairpin or a pseudo-knot, or may be part of a protein−nucleic acid complex. The poor catalytic activity of ANG may have evolved to maximize specificity for the target substrate. Hence, the identification of its physiological substrate is essential for the complete description of the mechanism by which ANG promotes angiogenesis.

ACKNOWLEDGMENT

We are grateful to Promega Corp. for providing a cDNA for human ANG and to Dr. R. Shapiro for insightful comments on the manuscript.

REFERENCES

1. Coulomb, C. A. (1884) *Collection de Mémoires Relatifs a la Physique*, Gauthier-Villars, Paris.
2. Gillmor, C. S. (1971) *Coulomb and the Evolution of Physics and Engineering in Eighteenth-Century France*, Princeton University Press, Princeton, NJ.
3. Folkman, J. (1971) *N. Engl. J. Med. 285*, 1182−1186.
4. Folkman, J. (1995) *Nat. Med. 1*, 27−31.
5. Ferrara, N., and Alitalo, K. (1999) *Nat. Med. 5*, 1359−1364.
6. Mousa, S. A. (2000) *Angiogenesis Inhibitors and Stimulators: Potential Therapeutic Implications*, Landes Bioscience, Georgetown, TX.

7. Folkman, J., and Klagsbrun, M. (1987) *Science 235*, 442−447.
8. Schott, R. J., and Marrow, L. A. (1987) *Cardiovasc. Res. 27*, 1155−1161.
9. Folkman, J., and Shing, Y. (1992) *J. Biol. Chem. 267*, 10931−10934.
10. Shapiro, R., Riordan, J. F., and Vallee, B. L. (1986) *Biochemistry 25*, 3527−3532.
11. Riordan, J. F. (1997) in *Ribonucleases: Structures and Functions* (D'Alessio, G., and Riordan, J. F., Eds.) pp 445−489, Academic Press, New York.
12. Strydom, D. J. (1998) *Cell. Mol. Life Sci. 54*, 811−824.
13. Badet, J. (1999) *Pathol. Biol. 47*, 345−351.
14. Fett, J. W., Strydom, D. J., Lobb, R. R., Alderman, E. M., Bethune, J. L., Riordan, J. F., and Vallee, B. L. (1985) *Biochemistry 24*, 5480−5486.
15. Shapiro, R., Strydom, D. J., Olson, K. A., and Vallee, B. L. (1987) *Biochemistry 26*, 5141−5146.
16. Strydom, D. J., Fett, J. W., Lobb, R. R., Alderman, E. M., Bethune, J. L., Riordan, J. F., and Vallee, B. L. (1985) *Biochemistry 24*, 5486−5494.
17. Raines, R. T. (1998) *Chem. Rev. 98*, 1045−1065.
18. Harper, J. W., and Vallee, B. L. (1989) *Biochemistry 28*, 1875−1884.
19. Shapiro, R., Fox, E. A., and Riordan, J. F. (1989) *Biochemistry 28*, 1726−1732.
20. Shapiro, R., and Vallee, B. L. (1989) *Biochemistry 28*, 7401−7408.
21. Raines, R. T., Toscano, M. P., Nierengarten, D. M., Ha, J. H., and Auerbach, R. (1995) *J. Biol. Chem. 270*, 17180−17184.
22. Shapiro, R., Harper, J. W., Fox, E. A., Jansen, H.-W., Hein, F., and Uhlmann, E. (1988) *Anal. Biochem. 175*, 450−461.
23. Leland, P. A., Schultz, L. W., Kim, B.-M., and Raines, R. T. (1998) *Proc. Natl. Acad. Sci. U.S.A. 98*, 10407−10412.
24. De Bernardez-Clark, E., Schwarz, E., and Rudolph, R. (1999) *Methods Enzymol. 309*, 217−236.
25. Pace, C. N., Vajdos, F., Fee, L., Grimsley, G., and Gray, T. (1995) *Protein Sci. 4*, 2411−2423.
26. Shapiro, R., and Vallee, B. L. (1991) *Biochemistry 30*, 2246−2255.
27. Blank, A., Sugiyama, R. H., and Dekker, C. A. (1982) *Anal. Biochem. 120*, 267−275.
28. Ribó, M., Fernández, E., Bravo, J., Osset, M., Fallon, M. J. M., de Llorens, R., and Cuchillo, C. M. (1991) in *Structure, Mechanism and Function of Ribonucleases* (de Llorens, R., Cuchillo, C. M., Nogués, M. V., and Parés, X., Eds.) pp 157−162, Universitat Autónoma de Barcelona, Bellaterra, Spain.
29. Kim, J.-S., and Raines, R. T. (1993) *Protein Sci. 2*, 348−356.
30. Bravo, J., Fernández, E., Ribó, M., de Llorens, R., and Cuchillo, C. M. (1994) *Anal. Biochem. 219*, 82−86.
31. delCardayré, S. B., Ribó, M., Yokel, E. M., Quirk, D. J., Rutter, W. J., and Raines, R. T. (1995) *Protein Eng. 8*, 261−273.
32. Laemmli, U. K. (1970) *Nature 227*, 680−685.
33. Kelemen, B. R., Klink, T. A., Behlke, M. A., Eubanks, S. R., Leland, P. A., and Raines, R. T. (1999) *Nucleic Acids Res. 27*, 3696−3701.
34. Park, C., Kelemen, B. R., Klink, T. A., Sweeney, R. Y., Behlke, M. A., Eubanks, S. R., and Raines, R. T. (2001) *Methods Enzymol. 341*, 81−94.
35. Ellis, K. J., and Morrison, J. F. (1982) *Methods Enzymol. 87*, 405−425.
36. Park, C., and Raines, R. T. (2001) *J. Am. Chem. Soc. 123*, 11472−11479.
37. Record, M. T., Jr., Lohman, T. M., and de Haseth, P. (1976) *J. Mol. Biol. 107*, 145−158.
38. Zhang, W., Bond, J. P., Anderson, C. F., Lohman, T. M., and Record, M. T. (1996) *Proc. Natl. Acad. Sci. U.S.A. 93*, 2511−2516.
39. Fisher, B. M., Ha, J.-H., and Raines, R. T. (1998) *Biochemistry 37*, 12121−12132.
40. Wada, K., Wada, Y., Doi, H., Ishibashi, F., Gojobori, T., and Ikemura, T. (1991) *Nucleic Acids Res. 19*, 1981−1986.
41. Witzel, H. (1963) *Prog. Nucleic Acid Res. 2*, 221−258.
42. del Rosario, E. J., and Hammes, G. G. (1969) *Biochemistry 8*, 1884−1889.
43. Park, C., and Raines, R. T. (2000) *FEBS Lett. 468*, 199−202.
44. Fisher, B. M., Grilley, J. E., and Raines, R. T. (1998) *J. Biol. Chem. 273*, 34134−34138.
45. Fisher, B. M., Schultz, L. W., and Raines, R. T. (1998) *Biochemistry 37*, 17386−17401.
46. Studier, F. W., Rosenberg, A. H., Dunn, J. J., and Dubendorff, J. W. (1990) *Methods Enzymol. 185*, 60−89.
47. Kim, J.-S., and Raines, R. T. (1993) *J. Biol. Chem. 268*, 17392−17396.
48. Leland, P. A., Staniszewski, K. E., Kim, B.-M., and Raines, R. T. (2001) *J. Biol. Chem. 276*, 43095−43102.
49. Spanjaard, R. A., and van Duin, J. (1988) *Proc. Natl. Acad. Sci. U.S.A. 85*, 7967−7971.
50. Kane, J. F., Violand, B. N., Curran, D. F., Staten, N. R., Duffin, K. L., and Bogosian, G. (1992) *Nucleic Acids Res. 20*, 6707−6712.
51. Rosenberg, A. H., Goldman, E., Dunn, J. J., Studier, F. W., and Zubay, G. (1993) *J. Bacteriol. 175*, 716−722.
52. Yoon, J. M., Kim, S. H., Kwon, O. B., Han, S. H., and Kim, B. K. (1999) *Biochem. Mol. Biol. Int. 47*, 267−273.
53. Markley, J. L. (1975) *Biochemistry 14*, 3546−3553.
54. Quirk, D. J., and Raines, R. T. (1999) *Biophys. J. 76*, 1571−1579.
55. Lequin, O., Thüring, H., Robin, M., and Lallemand, J.-Y. (1997) *Eur. J. Biochem. 250*, 712−726.
56. Leonidas, D. D., Shapiro, R., Allen, S. C., Subbarao, G. V., Veluraja, K., and Acharya, K. R. (1999) *J. Mol. Biol. 285*, 1209−1233.
57. Russo, N., Acharya, K. R., Vallee, B. L., and Shapiro, R. (1996) *Proc. Natl. Acad. Sci. U.S.A. 93*, 804−808.
58. Russo, N., Shapiro, R., Acharya, K. R., Riordan, J. F., and Vallee, B. L. (1994) *Proc. Natl. Acad. Sci. U.S.A. 91*, 2920−2924.
59. Messmore, J. M., Fuchs, D. N., and Raines, R. T. (1995) *J. Am. Chem. Soc. 117*, 8057−8060.
60. Nogués, M. V., Vilanova, M., and Cuchillo, C. M. (1995) *Biochim. Biophys. Acta 1253*, 16−24.
61. Acharya, K. R., Shapiro, R., Allen, S. C., Riordan, J. F., and Vallee, B. L. (1994) *Proc. Natl. Acad. Sci. U.S.A. 91*, 2915−2919.
62. Shapiro, R. (1998) *Biochemistry 37*, 6847−6856.
63. Albery, W. J., and Knowles, J. R. (1976) *Biochemistry 15*, 5631−5640.

BI0117899